ISSN-1996-918X





Pak. J. Anal. Environ. Chem. Vol. 25, No. 2 (2024) 200 – 213

http://doi.org/10.21743/pjaec/2024.12.03

Activated Carbon-Based Ormosils for Abatement of Uremic Toxins from Aqueous Solution and Blood Plasma Samples

Muhammad Arslan, Suryyia Manzoor, Tariq Mahmood Ansari* and Ghazala Yasmeen

Institute of Chemical Sciences, Bahauddin Zakariya University, Multan 60800, Pakistan.
*Corresponding author Email: drtariq2000@gmail.com
Received 10 April 2023, Revised 06 September 2023, Accepted 03April 2024

Abstract

The kidney is a vital human organ. Kidney diseases are associated with the accumulation of toxins in the body. If these toxins are not removed from the body create serious health issues, organ failure even death. Formulation or synthesis of material that can adsorb or detect these toxins from blood is very important. Herein, we report the synthesis of organically modified silanes incorporated with activated carbon particles (Silane-C). Afterwards, these particles were applied for the removal of creatinine and uric acid by adsorption from blood samples. Silane-C particles were characterized by Fourier Transform Infrared Spectroscopy, which indicated the presence of Si-O-C and O-Si confirmed the silane formation and polymerization. Moreover, the silane-C particles have a surface area of 249.3 m²g⁻¹. The SEM analyusis showed silane-chas groves and rough spongy edges surface. The thermogravimetric analysis depicted the weight loss percentage of silane-C particles was 8.4% and Energy Dispersive X-ray analysis demonstrated the presence of carbon, silicon, and oxygen atoms in particles with an abundance of 72.4, 16.0, and 10.9, respectively. The binding capacity of silane-C particles to remove creatinine and uric acid from blood was 117 and 44 mgg⁻¹, respectively. Percentage recovery for both toxins was observed up to 90%. The RSD (1.03%), LOD (8.8 $\times 10^{-2} \,\mu gmL^{-1}$) and LOQ (2.8 $\times 10^{-1} \,\mu gmL^{-1}$) were calculated from signal-to-noise ratio for uric acid. The removal process followed the Langmuir adsorption isotherms. The RSD (1.11%), LOD (9.3 $\times 10^{-2} \, \mu \text{gmL}^{-1}$), and LOQ (3.1 $\times 10^{-1} \, \mu \text{gmL}^{-1}$) were calculated from signal-to-noise ratio of HPLC for creatinine, but the removal of creatinine followed Freundlich adsorption isotherm. These results demonstrate the ability of synthesized material to work as an efficient adsorbent for the removal of creatinine and uric acid from blood samples.

Keywords: Blood samples, Uric acid, Silane-C, Creatinine

Introduction

Due to substandard diets and sedentary lifestyles, chronic kidney diseases (CKD) in humans are increasing day by day. The prevalence of chronic kidney diseases is 31% in Pakistan. In healthy people, toxins are removed through the body by kidneys but in patients with CKD, these accumulate in the bloodstream. Due to COVID-19,admitted patients' frequency of kidney diseases has

increased. People suffering from kidney disease necessarily endure hemodialysis sessions three times a week, every time-consuming abundant water (120 L)[1-4]. The waste of Ultra-pure water is the biggest obstacle in the miniaturization of hemodialysis. This probation has put direct pressure on the supply of materials for dialysis and led the doctors/scientists to search for

efficient materials. Different methods have been introduced by the researchers to minimize the wastage of water by computing their generation process, which includes sorbents having layers, salts of zirconium, and activated carbon for ablation of creatinine, urea, and uric acid [5-10]. Due to high solubility and smaller molecular sizes creatinine uric acid are delicate and components to remove. Even high-fluxed dialysis machines can remove 60 to 75% of creatinine and uric acid from blood. A higher amount of these toxins in the body causes diseases including muscular several dystrophy, diabetic nephropathy, and more serious renal collapse [11-13]. For normal performance, these toxins must be removed from the body. Among currently used substances, porous materials manifested as good adsorbents and showed promising results in the removal of uremic toxins. Metal-organic frameworks have shown their ability in adsorption due to high porosity, and wide surfaces are often found used in catalysis, sensors [14,15], energy conversion, and storage industries. The presence of metal ions can induce allergic reactions or sensitivity. Hence use of metal organic frameworks (MOFs) is also compromised. Moreover, activated carbons have been used since 1969 because they are considered good adsorbents due to their arranged pore sites and controllable surface area. The complex synthesis process, high cost, and low selectivity are reasons to find some other efficient adsorbents. In the recent past organically modified silanes (ORMOSILS) and activated carbon have been widely used for the removal of pollutants and toxins. ORMOSILS are preferred because their structures can be manipulated according to the affinity of the analyte. These particles have symmetrical channels and slender pore dispersion. Limitations of silica include inertness, hydrothermal solubility, and lower mechanical strength. However. these

limitations can easily be removed modification of silica with different functional groups. Herein, we prepared a hybrid material in which silica from tetraethyl orthosilicate (TEOS) and activated carbon particles were coupled in Methacryllic acid polymer with vinvltriethoxv silane (VTEOS). adsorption capacity, immunizing inertness, low cost, and high manoeuvrability in pore size and surface functionalities of these particles make them a novel material which has not been synthesized and used for the removal of uremic toxins before. This modification increases the affinity adsorbent for toxins, reusability, mechanical strength, and hydrothermal stability. These properties are the reason for the selection of Methacrylic acid polymer by activated carbon hybrid particles for abatement of creatinine and uric acid from blood samples.

Materials and Methods Reagents and Chemicals

Uric acid (98%), Hydrochloric acid (37%), Sodium hydroxide (65%), Perchloric acid(70%). Potassium hvdroxide. Creatinine (98%) were purchased from Merck (Darmstadt, Germany). Tetraethylorthosilicate (97%), Vinyltriethoxy silane (97%), and Lithium acetate (99%) of Sigma (St. Louis, USA) were used. Methacrylicacid from Duksan Anson, South Korea with 99% purity. Benzoyl peroxide, lithium chloride, Acetic acid (99%), Sodium acetate (99%), Methanol (99.9%), and Activated carbon (85%) were purchased from Dae-Jung (Siheung, South Korea).

Instruments

High-Performance Liquid Chromatography (HPLC) analysis was performed using the LC-20AT model of Shimadzu, Japan having an ultraviolet-visible spectrophotometer detector and an Agilent C18 column with an internal diameter of 4.6 mm, a length of 250 mm, and a particle size of 5.0 μ m. Pyrex glassware was used for all the research work. Weighing analytical balance model no. AB204 Mettler Toledo having range from 0.001 to 200 g was used. Whatman filter paper no. 42 was used for the filtration of samples and the filtration of the mobile phase 0.25 μ m was used. Electro analytical weiging balance balance Shimadzu UX2200H Japan. Benchtop pH meter from Hanna instruments (USA), model (HI-2211) was used for pH measurement.

Synthesis of Silane-C Particles

5 mL of vinyltriethoxy silane (VTEOS) and 5 mL methacryllic acid (MA) were mixed in a round bottom flask. Then, 10 mg of benzoyl peroxide acting as an initiator was also added to that mixture. This mixture was kept in an inert environment by closing the neck of the flask with a nitrogen-filled balloon on a hotplate in a paraffin bath. A constant stirring at 2500 rpm and 80 °C temperature was kept until turbidity in the mixture appeared. This was marked as flask "A". In another round bottom flask marked as "B", Tetraethylorthosilicate (TEOS) (5 mL) and 0.5 g of activated carbon were kept stirred at 2500 rpm to get homogenized mixture. 2 mL of dilute HCl (0.1 M) was added to this mixture. At the moment when turbidity appeared in flask "A", the mixture from flask "B" was poured instantaneously into flask "A". After that, this flask was stirred continuously at 2500 rpm, and 80 °C was maintained until silane-C particles were prepared.

Characterization

Fourier transform infrared (FTIR) spectrum of silane-C composite was obtained using Bruker Alpha-11 spectrometer (Billerica, MA, USA) in the range (4000-400) cm⁻¹. Scanning electron microscopy (SEM) of

Hitachi (Tokyo, Japan) was used for surface characteristics elucidation. Surface area, pore volume, and pore sizes of silane-C particles were calculated by using the Brunauer-(BET) technique Emmett-Teller Thermo Gravimetric Analysis (TGA) and Differential Scanning Calorimetry (DSC) were used to investigate thermal stability and physical changes in prepared material. Universal V4.5 A T.A. instrument (25-1000 °C) at 5 °C min⁻¹ from Perkin Elmer (USA) to analyze silane and water content in synthesized material. Energy Dispersive X-Ray model EDX-7200 AI13-U92 by Rigaku (USA) was used for elemental percentage. Elecroanalytical balance of Hawach Scientific (China) was used for weighing different samples. Benchtop pH meter model 7110 from CarLoth (USA) was used.

Adsorption Studies

HPLC (SPDA-20A and E2695), having reverse phase C-18 column and ultravioletvisible detector was used for the detection of analytes. At room temperature batch adsorption studies were evaluated. Optimization of adsorption variables like time of contact, amount of analyte, pH, and dose of adsorbent was done by varying one factor and keeping all other conditions the same. Zero charge pH point of adsorbent was also measured. Maximum qe (Amount of analyte adsorbed on adsorbent in mgg⁻¹) value indicates optimum conditions for all factors. Adsorption isotherms were applied to investigate the adsorption behavior of silane-C particles.

Real Sample Analysis

An official approval from the departmental Ethical Research Committee was acquired to analyze blood samples. Blood samples of patients suffering from kidney diseases were collected. Plasma was kept in liquid nitrogen till analysis.3 mL plasma was

added to 5 mL of dilute perchloric acid (1 M) and centrifuged at 4000 rpm for 15 minutes. Solid residues were discarded, and the supernatant was neutralized by cold potassium hydroxide (2M) [16]. This vortex process enabled the removal of the protein part of the plasma. 10 mL of this liquid spiked by 100 mgL⁻¹ of creatinine and 40 mgL⁻¹ of uric acid separately. Both solutions of creatinine and uric acid wereused for adsorption under optimized conditions.

Regeneration Studies

The chemical regeneration process was used to reduce the cost and time of production. The efficiency of the regeneration process depends on different factors including the substitution of active site, nature of pores structures, adsorption method, functional groups, etc. In the regeneration industry, the secondary contamination process is a crucial challenge that is faced. For this material regeneration of material was observed by desorption of the analyte by chemicals and reused for adsorption in the next cycle. Creatinine and uric acid adsorbed on silane-C can be desorbed by treating with 10 mmolL⁻¹ acetic acid and 30 mmol L⁻¹ lithium chloride.

Results and Discussions Surface and Functional Characterization of Silanes-C Particles

Fig. 1 shows the FTIR spectrum of various functionalities that are involved in interaction with the analytes and serving as active sites for adsorption. Peaks at 1054 cm⁻¹ and 820 cm⁻¹ are due to stretching vibration of Si-O-C and O-Si, respectively. The gel of TEOS and VTEOS condensed on activated carbon which indicates successful grafting. Si-O functional groups are represented by peaks at 1033cm⁻¹. The stretching bandof the carboxyl group appeared at 1720 cm⁻¹. 2973 cm-1 and 2952 cm-1 in the spectrum

represents stretching of aliphatic groups in Silane-C particles. The broad peak at 3450 cm⁻¹appeared to be water molecules presenting silane-C particles [17].

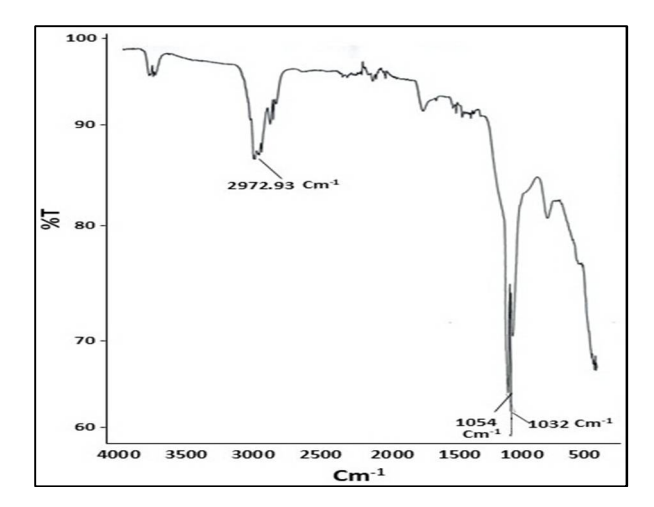


Figure 1. FTIR spectrum of silane-C particles

The surface morphology of Silane-C was also explored by SEM. In Fig. 2 under SEM scans of silane-C particles look like grains of sand with unevenly sharp edges. Divergent sizes of particles are due to the rough condensation of ORMOSIL. Scratches on the surface of activated carbon appeared due to the attachment of silica gel layers. Activated carbon is strongly nucleated by gels. It is also observed that the surface of the particles had groves and rough spongy edges. A closer look at the images (Fig. 2) suggested the presence of a porous structure. All these modifications of particles enable enhancement of surface-active sites. Hence good adsorbent materials are likely to be obtained.

Scan of EDX of silane-C particles (Fig.3) demonstrates the presence of carbon, silicon, and oxygen atomsin particles. Atomic % of C, O, and Si in silane-C particles was found 72.4, 16.0, and 10.91%, respectively. Furthermore, the weight % of C, O, and Si in silane-C particles was found as 59.9, 17.6, and 21.1%, respectively.

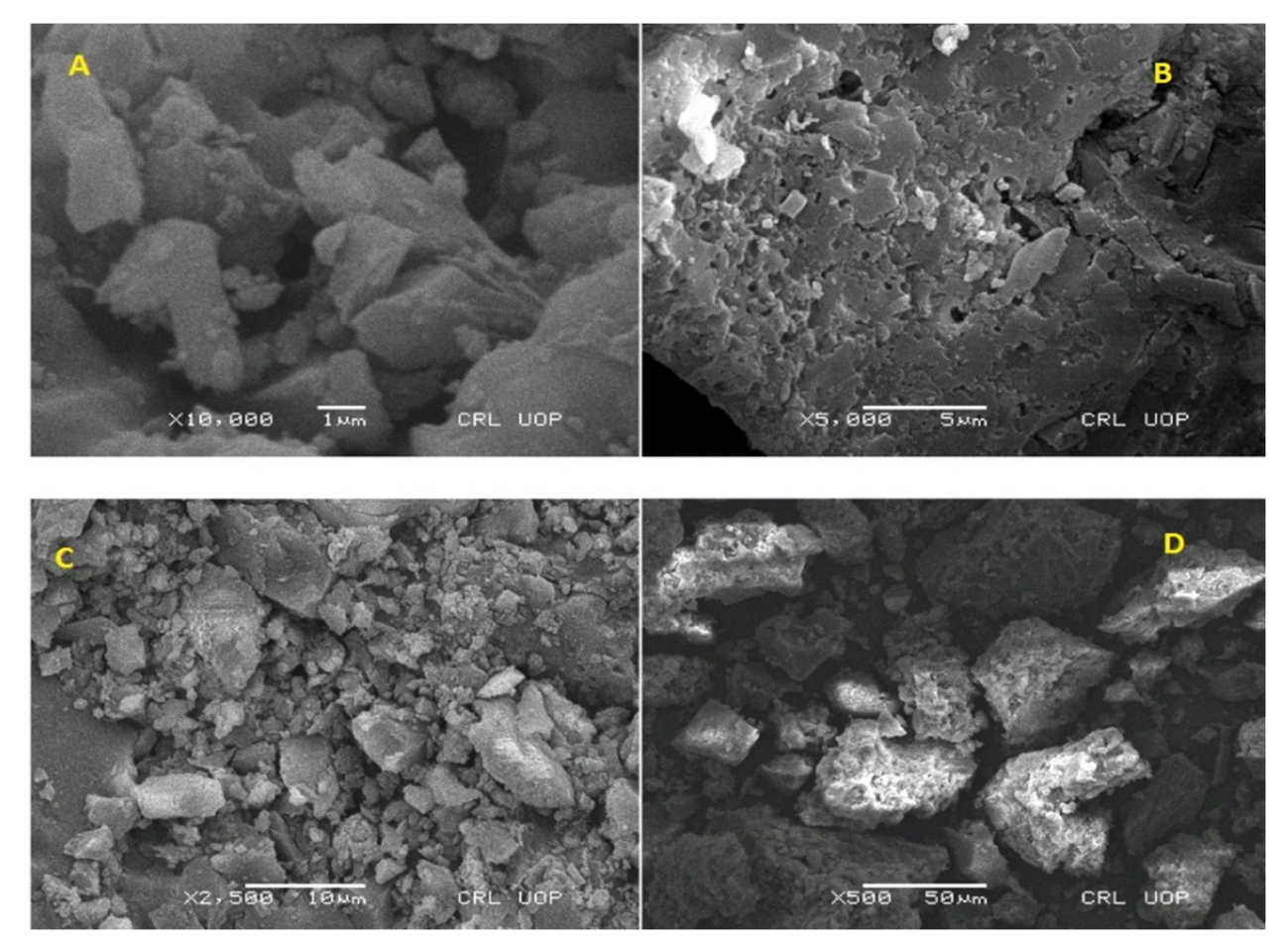


Figure 2. SEM images of silane-C particles (A) 1 μm, (B) 5μm, (C) 10 μm, and (D) 50 μm

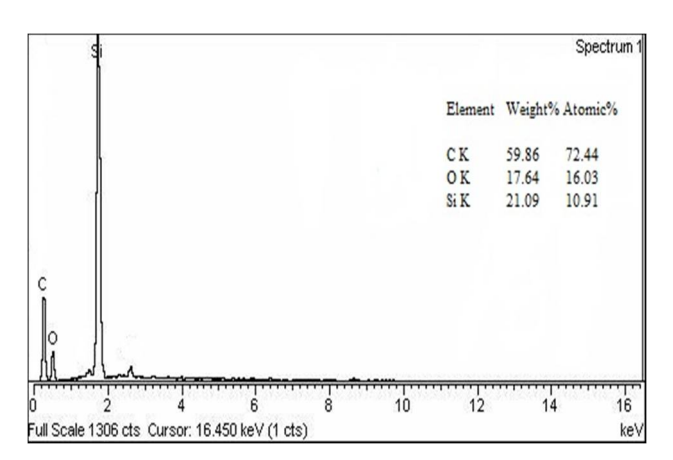


Figure 3. Energy Dispersive X-Ray Analysis (EDX) of silane-C narticles

Pores dimensions and surface area of particles can be determined by BET. The results of the Silanes-C particles are discussed below in Table 1. The availability of microspores on the surface of synthesized

material was confirmed due to uptake at lower pressure. The average width of the pore was $20.9\,\text{ Å}\,$ (4V/A). Pore volume and external surface area of porous material are mostly calculated by t-plot. The thickness curve and standard isotherm represent the adsorption due to adsorptive film and smooth reference site. The external area on the t-plot for silane-C was $63.3\,\text{m}^2\text{g}^{-1}$.

Table 1. Results of BET surface characterization of silane-C.

Parameters	Results
Surface Area	249 m ² g ⁻¹
Langmuir Surface Area	$347 \text{ m}^2\text{g}^{-1}$
Microspore Area	$187 \text{ m}^2\text{g}^{-1}$
T-Plot External Surface Area	$63.3 \text{ m}^2\text{g}^{-1}$
Micropore volume	$0.091~{\rm cm^3 g^{-1}}$

TGA (Fig. 4) shows that the weight loss below 120 °C is because of water loss, and deposition due to vicinal silanol group condensation in non-volatilized solvent. The weight loss percentage of silane-C particles in this temperature range was 8.4%. Further loss between 120-400 °C is because slightly higher temperature has attributed to the detachment of physically adsorbed silane; weight loss was 7.1%. Moreover, peaks between 400 - 425 °C are due to oxidation, and the total loss of silane weight - in this region was 24.9%. An upward peak of DSC is indication of exothermic reaction. Residual organic compound burning in start could be reason behind exothermic reaction and relatively flat line after 600-1000 °C is related to stability of activated carbon to thermal degradation. Exothermic peak from 200-500 °C shows oxidation of organic components, decomposition of organic- inorganic bond above this exothermic peak is because of phase transition.

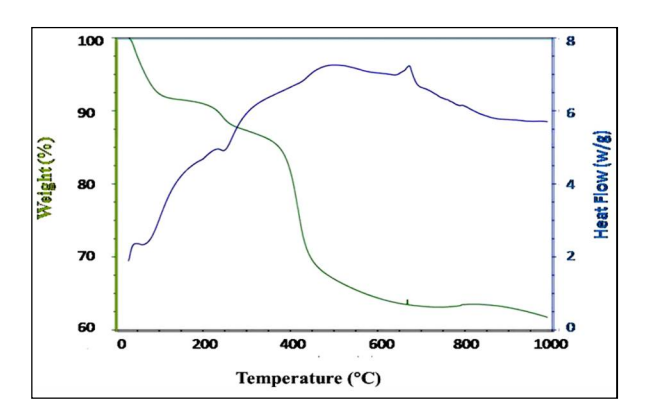


Figure 4. Thermo Gravimetric Analysis (TGA) and Differential Scanning Calorimetry of silane-C particles

Adsorption Studies

Adsorption of creatinine on silane-c particles can be described as follows: The driving forces in the adsorption of creatinine are Van Der Waal forces. Electronegativity difference in atoms of creatinine produces a dipole in each molecule. The dipole of creatinine molecule and dipole induced in

silane-C particles cause dipole-dipole-induced interaction, so creatinine molecules adsorbed on the surface of silane-C particles. The dipole of oxygen on the surface of creatinine and the dipole of silane-C particles also considered for dipole-dipole interaction adsorption. Hydrogen bonding between surface hydrogen atoms andother electronegative atoms of creatinine and silane-C particles is also involved in the adsorption process. Multilayer adsorption of creatinine is facilitated by hydrogen bonding between new molecules and already adsorbed creatinine. In the case of uric acid adsorption on silane-C particles including above mentioned forces, there is an addition of hydrophobic interaction between uric acid and silane-C particles. Different active sites present on the surface of synthesized materials arefunctional groups such as -Si-O, -OH, C-Si,-COOH, and silanol. Three different types of forces are involved in the attachment of toxins with silane-C particles: (a) coordination bonding, hydrogen bonding, (c)electrostatic affinity, hydrophobic and hvdrophilic (d) interaction. Ionic natures of toxins facilitate the removal capacity of these hybrid materials. The amount of analyte adsorbed on the adsorbent can be calculated by drawing a calibration curve. Standard solutions were prepared for the calibration curve. The amount of toxin adsorbed and percentage removal by silane-C particles can calculated by equations [18] given below:

$$q_e = (rac{C_i - C_e}{M}) \ V$$

Percentage Removal = $(rac{C_i - C_e}{C_i}) imes 100\%$

 C_e = Equilibrium concentration of analyte q_e =Amount of analyte adsorbed on adsorbent in mgg⁻¹

 C_i = Initial concentration of analyte M=Mass of adsorbent in gram

V= Volume of analyte solution in a litre

Optimization of Adsorption Parameters

To improve adsorption capacity, optimization of parameters was carried out. It has been observed that the uptake of toxins increases spontaneously with the increase in time of contact (Fig. 5). Large pore size and pore volume can be attributed to this sudden increase in uptake. An increase in contact time to 60 minutes resulted in 90% removal of toxins however further time increase led to a decrease in the removal of toxins. This decrease may be due to the desorption of toxins from silane-C particles. Creatinine and uric acid removal increased with the increase in adsorbent amount, this is directly related to the number of available active sites. Removal efficiency increased with increasing

concentration of the toxins up to some extent and then stopped due to a fixed amount of adsorption sites against an increased number of toxins molecules and establishment of chemical equilibrium. Adsorption is also increased with increasing pH the highest removal is near neutral pH.

Adsorption of creatinine and uric acid is increased till the attainment of reaction equilibrium. This is directly related to active sites available for attachment of analyte. The large surface area of silane-C particles is highly favorable for the removal of creatinine and uric acid. Even though it was highly soluble and smaller in size, these toxins were efficiently separated.

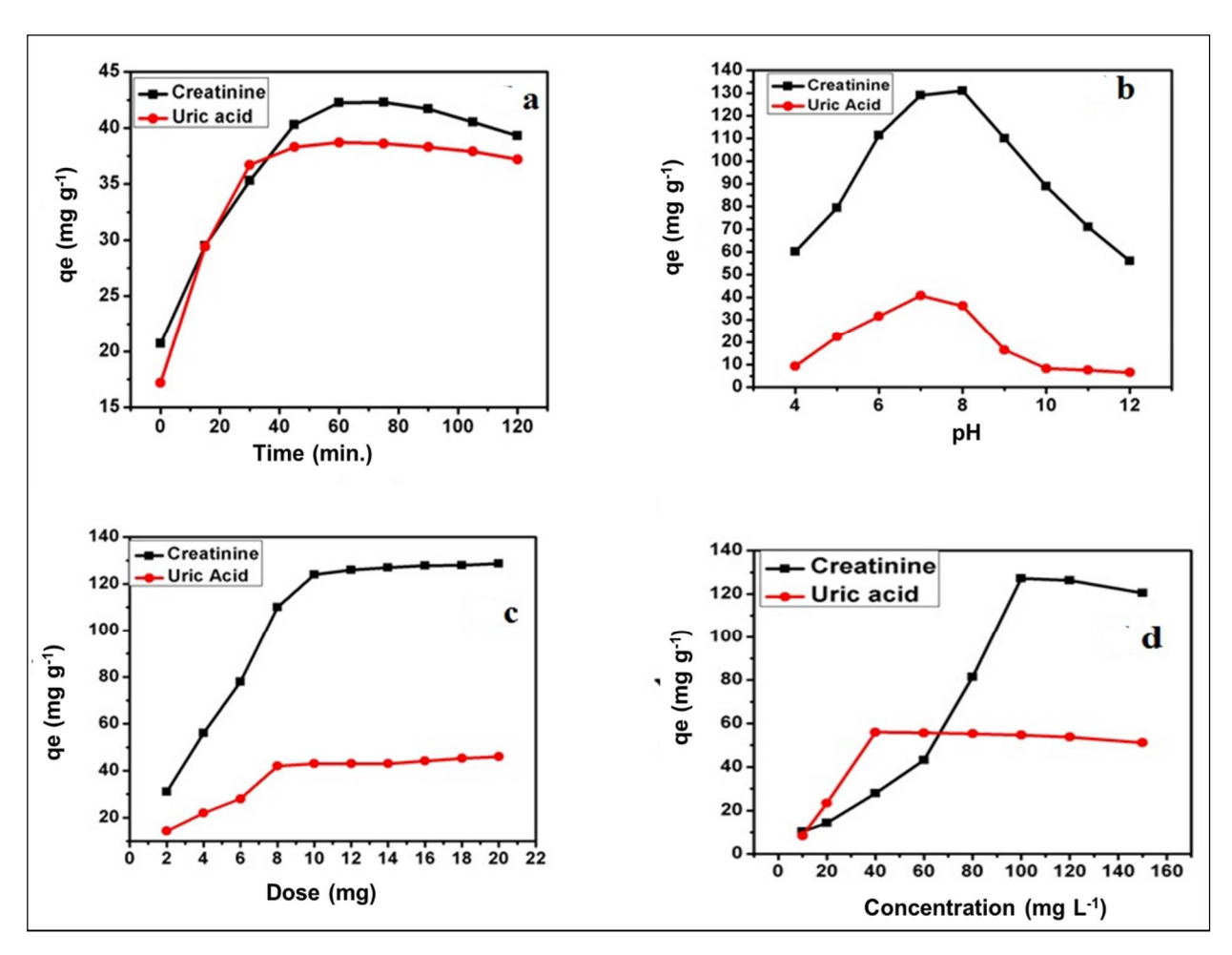


Figure 5. Effect of time (a), pH (b), adsorbent dose (c), and concentration of analyteson adsorption (d)

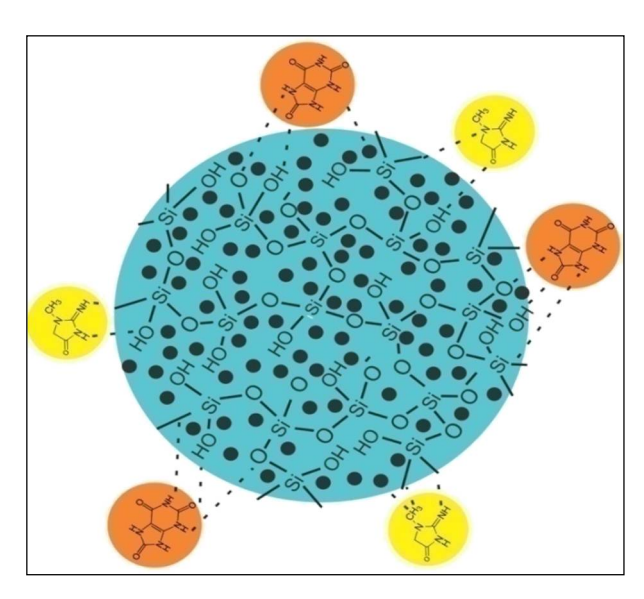


Figure 6. Adsorption mechanism of creatinine and uric acid on silane-C particles

Amine and imine are possible forms of two tautomers of creatinine, but there is domination of amine in solution form [19, 20]. Creatinine is protonated in an acidic medium pKa for creatinine is 4.4 but at 7 pH it is neutral [21]. In an acidic medium protonated creatinine is adsorbed on silane-C particles, while the neutral form of creatinine is when passed through pores and ridges of silane-C particles it gets protonated and adsorbed. Hydrogen bonding is another main factor involved in the attachment of creatinine with adsorbent. As discussed above in aqueous solutions amine form of creatinine dominating. Hydrogen attached toN* involved in primary hydrogen bonding. Protonation of creatinine occurs at N* while deprotonation at N** [22].

Uric acid is also found in two tautomeric forms. Tautomer equilibrium exists between uric acid, 2, 4, 6, trihydroxy purine [23]. This equilibrium can be shifted to either direction depending upon conditions. In acidic conditions, it is present as uric acid but in the basic medium, it is present as purine-oxygen ion and 2,4,6-trihydroxy purine. In neutral conditions, uric acid may be present inall three forms. Adsorption of uric acid on silane-C

particles is related to hydrogen bonding and interaction. Three electrostatic hydroxyl groups and N atoms in uric acid are involved in hydrogen bonding with silane-C particles. Electrostatic interaction between positive charges of silane-C particles and negative charge of purine-oxygen molecules is also reason behind adsorption. The highest adsorption of uric acid was observed at neutral pH. Variations in pH cause changes in the behaviors of uric acid and adsorbent moreover forces involved in adsorption also change. This adsorption mechanism is shown in Fig. 6. The hydrogen bonding and electrostatic interactions at low pH are poor because ofthe protonation of silane-C particles thepossibility purine-oxygen of ions. However. at basic conditions, more electrostatic interaction occurs because of purine-oxygen ions and hydrogen bonding. The highest adsorption takes place in a neutral environment because of hydrogen bonding chemical electrostatic interaction and attachment may also occur due to electrostatic interaction [24].

Zero Charge Point of pH

The point of zero charge is pH where the material surface has zero charge. At this point, a positive charge on the surface of materials is equal to a negative charge. The pHzc depends upon the surface of the material and chemistry in silane-C particles. In these particles, we used activated carbon and silanes. Modified silane surfaces usually have pHzc in the acidic range due to deprotonation of silanol groups (Si-OH). pHzc of activated carbon also lies in the acidic range. We used method for the mass titration the determination of the pHzc of silane-C particles. 50 mL of NaCl (0.5M) was taken in six different flasks. Every flask pH was adjusted to different pH (2, 4, 6, 8, 10, 12) using 0.1 M (HCl) and 0.1 M (NaOH) [25]. Then 0.5 g of adsorbent was added to each

flask. These flasks were shaken for 24 hours using a mechanical shaker. Each flask was filtered and change in pH was measured. A graph between the initial and final pH was drawn shown in Fig. 7. The point where the final pH line crossed the initial pH was the pHzc. In the case of silane-C particle, it was less than pH 3.

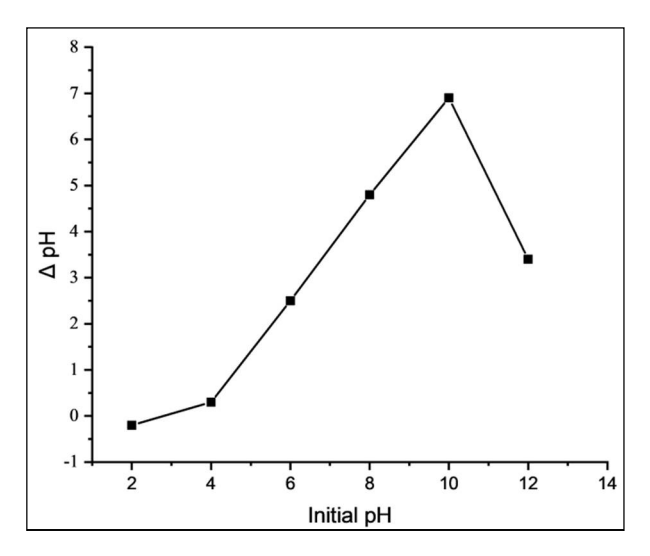


Figure 7. Plot between Δ pH and initial pH for the pHzc of silane-C particle

Adsorption isotherm

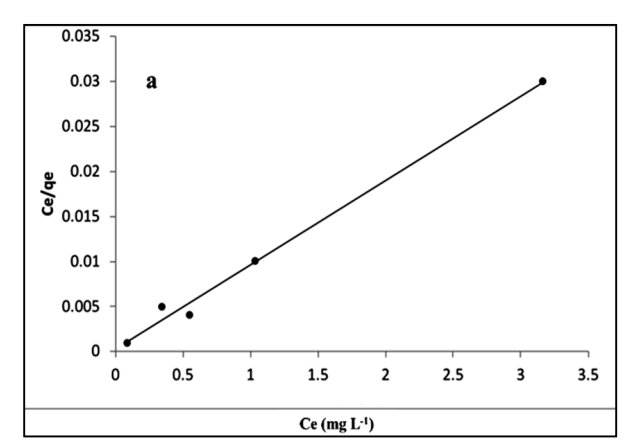
Two models Freundlich and Langmuir isotherms were discussed to investigate the behavior of creatinine and uric acid adsorption on silane-C particles. Langmuir isotherm shows the relation of the active site with the concentration of adsorbate molecules. Langmuir equation is given below:

$$\frac{C_e}{q_e} = \frac{1}{qb} + \frac{Ce}{q_0}$$

$$R_{L=} \frac{1}{1 + bC_i}$$

 C_e = Equilibrium concentration of analyte q_e = Analyte adsorbed on adsorbent in mgg⁻¹ q_0 = highest single layer removal in mgg⁻¹ b = Langmuir constant Lmg⁻¹

Langmuir isotherm can be plotted by taking C_e on the y-axis and C_e/q_e on the x-axis in Fig. 8 a and b,a straight line enables us to find different parameters. Separation factor " R_L " is represented as the supreme character to measure the validity adsorption phenomenon by this isotherm.



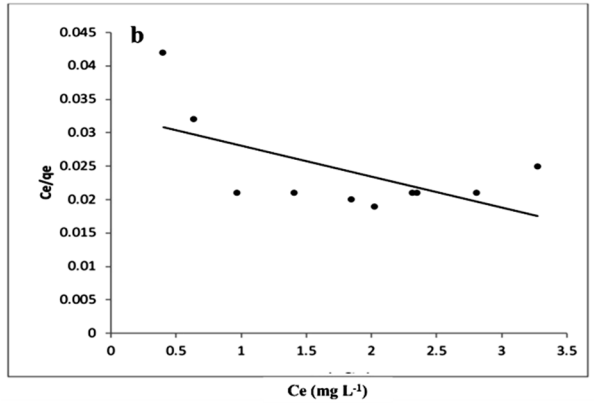


Figure 8. Langmuir isotherm graphical representations of creatinine (a) and uric acid (b)

Table 2. Langmuir and Freundlich adsorption plot data of toxins.

	Langmuir plot				Freundlich plot		
Toxin	B Lmg ⁻¹	q_o mgg^{-1}	R_L gL^{-l}	R^2	K_f	N	R^2
Creatinine			0.065	0.36	3.2634	0.669	0.9746
Uric acid	31.05	107.526	0.0003	0.9922	38.636	0.762	0.937

Freundlich isotherm enables us to deal with the limitation of the Langmuir plot in Fig. 9. This plot determines the relation between multilayer adsorption and varying concentration pressure. Equations are given below:

 $x/m = kP^{1/n}$ $\ln q_e = \ln K_f + \frac{1}{n} \ln C_e$ m = Adsorbent mass x = Analyte adsorbed 1/n = Adsorption effectiveness $K_f = \text{Adsorption capacity}$

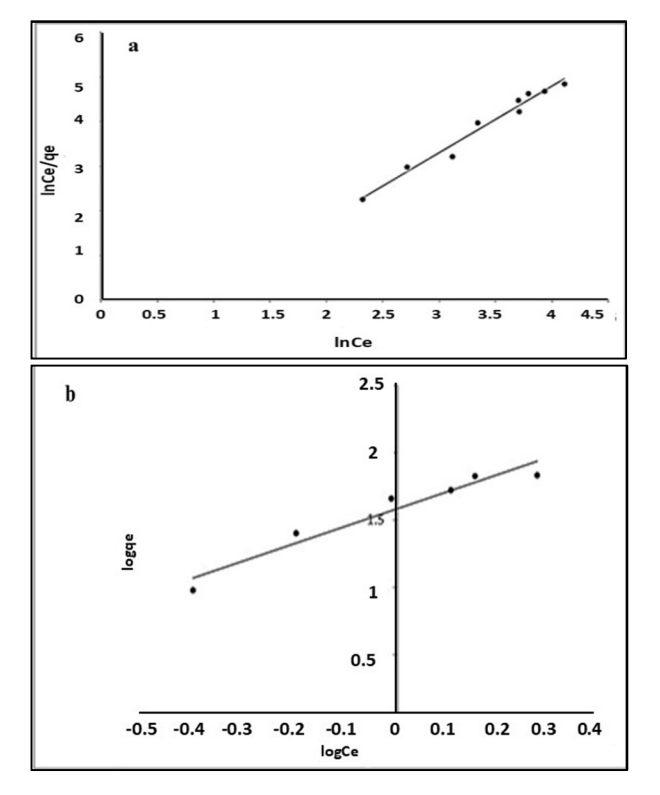


Figure 9. Freundlich isotherm graphical representations of uric acid (a) and creatinine (b)

At low pressure, the adsorption is linear but as concentration is increased then it follows Freundlich's adsorption isotherm. From the above data and R² values, it is clear that uric acid adsorption follows Langmuir adsorption isotherm, but creatinine fitted well the Freundlich adsorption isotherm model as in Fig. 8 and 9.The experimental adsorption capacity for these uremic toxins is almost near the calculated amount.

Reusability

The reusability of an adsorbent material is the key factor in decreasing production costs as well as wastage.

Creatinine and uric acid adsorbed on silane-C can be desorbed by treating with 10 mmolL ¹acetic acid and 30 mmol L⁻¹ lithium chlorides. In this work, we calculated the adsorption capability of synthesized particles using adsorption and desorption cycles 5 times on the same material. After five consecutive cycles, silanes-C particles for creatinine and uric acid have shown a very minute decrease in adsorption capacity from 90% to 82% and 88% to 80%, respectively. Hence this material can be used multiple times without any special treatment and a significant decrease in efficiency. The stability and rigidity of particles are clear Fig. 10. These results show that silane-C particle interactions are strong enough that activated carbon does not breach out even after treatment of 5 cycles.

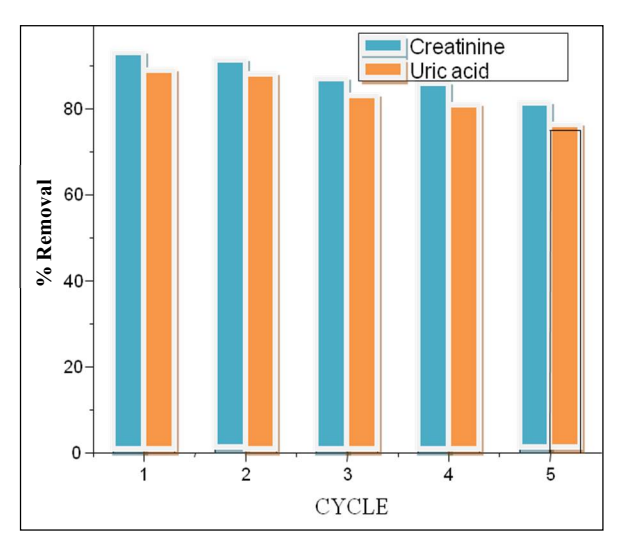


Figure 10. Reusability of Silane-C

The use of silane-C activated carbon biomedical applications necessitates for assessing the biocompatibility of these When in contact with blood, materials. materials may induce various side effects such cytotoxicity, hemolytic anaemia, thrombogenicity. However, silane-C hybrid materials not only exhibit high adsorption capacity, easy synthesis, and rapid adsorption demonstrate also good biocompatibility [28, 29].

Blood Plasma Analysis

During blood sample analysis, it is crucial to ensure that non-selective adsorption of certain beneficial ions and analytes to the adsorbent does not occur, as this can trigger adverse reactions, endangering the life of the patient. A 100 mgL⁻¹ standard solution of creatinine was prepared, and 9 mL of this solution was mixed with 1 mL of blood plasma to create a spiked working solution. Similarly, a 40 mgL⁻¹ standard solution of uric acid was prepared, and the spiked solution was made in the same manner. The HPLC conditions included using a mobile phase of 20 mmolL⁻¹ acetic acid, 1% methanol, and 30 mmolL⁻¹ sodium acetate. The analyte was filtered through a 0.45µm filter before injection. The UV-visible detector was set at a wavelength of 234 nm, with a run time of 4 minutes for each analysis. The concentration of the analyte was determined from the peak area of the chromatogram. The chromatogram for creatinine is shown in Fig. 11.

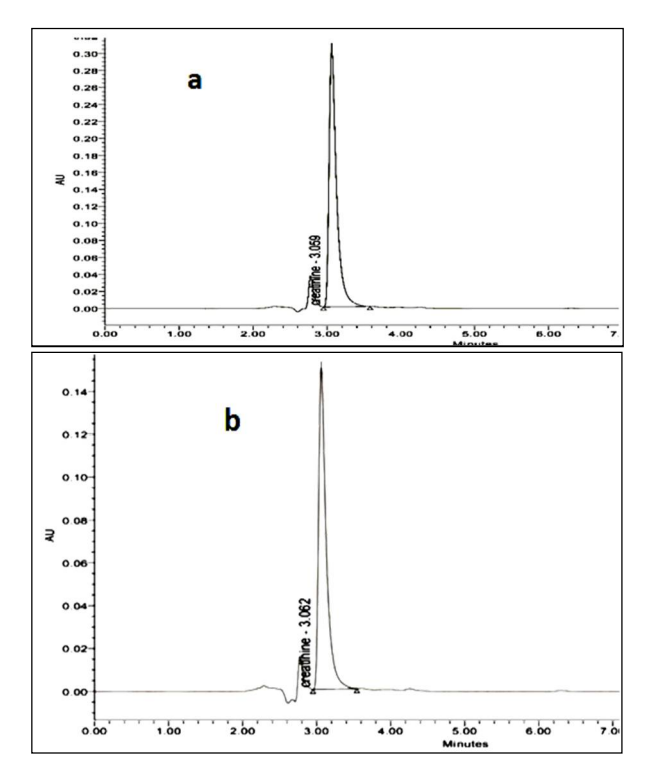


Figure 11. Creatinine chromatograms: (a) before adsorption and (b) after adsorption

A Chromatogram of spiked working analyte before and after adsorption clearly shows that 90% of creatinine is removed by silane-C particles. 117 mgg⁻¹ of creatinine adsorbed on adsorbent in one hour of contact time.

A lower concentration of uric acid was observed in blood plasma after deproteination. This may be due to its precipitation at lower pH.The spiked sample solution chromatogram for uric acid removal is shown in Fig.12. A 44 mg g⁻¹ of uric acid was removed by adsorbent material in 60 min. time duration.

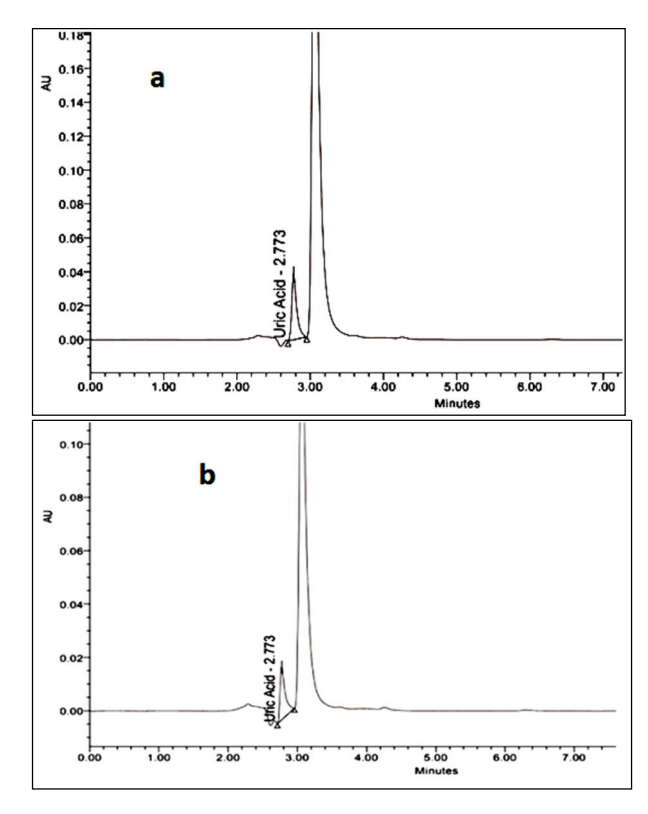


Figure 12. Uric acid chromatograms: (a) before adsorption and (b) after adsorption

Comparative study

Table 4 shows a list of different adsorbents used for the removal of creatinine and uric acid in recent years with percentage removal and adsorption capacity.

Table 4. Comparison of different adsorbents for removal of creatinine and uric acid.

Adsorbent	Creatinine q _e (mgg ⁻¹)	Uric acid q _e (mgg ⁻¹)	Reference
MoO ₃ -COOH	-	-	[3]
Zeolites	0.1260	-	[8]
Spherical activated carbon	20	20	[9]
MOF	30	-	[26]
poly (ethylene-co-vinyl alcohol) (EVOH)- zeolite-polymer composite nanofibers	25	-	[10]
Poly (ether sulfone)/activated carbon	83	-	[13]
UiO-66-(COOH) ₂ 83 PAN-U-60	83	-	[27]
83 PAN-U-60	54	-	[27]
Nylon-6/GNP/CB 0.50%	-	-	[15]
Silane-C	120	64	Present work

From comparison, it is obvious that silane—C particles synthesized in this work are very efficient from the adsorbent available these days. Higher amounts of toxins adsorbed on adsorbent in current work can be subjected to different properties like surface area, pore size stability, and sensitivity of silane-C particles. These particles have a modest surface area that can adsorb more molecules of toxins. A hybrid nature of silane-C particles also increased the broad range of toxin adsorption. Till now in our knowledge silane-C particles have superior uremic toxin removal efficiency, so can be used for hemodialysis or hemoperfusion studies.

Conclusion

The outcome of experimental analyses represents the higher efficiency and capacity of these silane-C particles in removing toxins. These particles were able to abate 120.29

mgg⁻¹ and 117.12 mgg⁻¹ of creatinine from standard solutions and blood respectively, whichis almost 90% in terms of percentage. Moreover, silane-C materials adsorb 63.2 and 44 mgg⁻¹of uric acid from standard solutions and blood samples, respectively. These values enable synthesized material to work as an efficient adsorbent for the purification of environmental and blood samples. In terms of percentage, we were able to remove creatinine and uric acid from blood samples by 90 and 84%, respectively. Hence silane-C particles proved good adsorbent that may be used removal ofother toxins environmental and blood samples in future studies. Highly porous adsorbents necessary to attain considerable adsorption so that can be used in clinical applications. Structural or functional modifications are applied to increase adsorption efficiency for certain molecules. To our knowledge, activated carbon-based silane-modified adsorbents stand out as the optimal solution for removing uric acid and creatinine. These poised materials are to revolutionize hemodialysis as dialysate materials by seamlessly addressing critical challenges such as biocompatibility and selectivity, all while maintaining their exceptional adsorption capacity.

Acknowledgement

This paper is a part of Ph.D thesis of Muhammad Arslan. The authors gratefully acknowledge the research facilities provided by the Institute of Chemical Sciences, Bahauddin Zakariya University, Multan, Pakistan, Drug Testing Laboratory, Kidney Center Multan, Pakistan, and Solex Chemical Industries Ltd. Multan, Pakistan. Ethical approval was obtained from the Institutional Research Ethical Committee of Bahauddin Zakariya University, Multan, Pakistan on 1st March 2021.

Conflict of Interest Statement

The authors declare that they do not have any conflict of interest regarding the research work presented in this manuscript.

References

- 1. V. Gura, M. B. Rivara, S. Bieber, R. Munshi, N. C. Smith, L. Linke, J. Kundzins, M. Beizai, C. Ezon and L. Kessler, *JCI Insight*, 1 (2016)565. https://doi.org/10.1172%2Fjci.insight.86397
- G. Lesaffer, R. De Smet, N. Lameire, A. Dhondt, P. Duym and R. Vanholder, Nephrol. Dial. Transplant., 15 (2000) 57.
 - https://doi.org/10.1093/ndt/15.1.50
- 3. R. Maleki, A. M. Jahromi, S. Mohaghegh, S. Rezvantalab, M. Khedri and L. Tayebi, *Appl. Surf. Sci.*, 566 (2021) 150629. https://doi.org/10.1016/j.apsusc.2021.15
- 4. J. Ahmed, S. Azhar, N. ul Haq, S. Hussain, A. Stájer, E. Urbán, M. Gajdács and S. Jamshed, *Int. J. Environ. Res. Public Health*, 19 (2022) 5015. https://doi.org/10.3390/ijerph19095015
- 5. K. Tharpa, P. Mahabala, C. Gurunath, J. Jose, S. Tantry, R. Choorikkat, D. Tymoshenko, H. de Brouwer and A. Kumar, *J. Artif. Organs.*, 23 (2020) 47. https://doi.org/10.1007/s10047-019-01131-5
- 6. S. R. Ash, Semin. Dial.,22(2009)615. https://doi.org/10.1111/j.1525-139X.2009.00657.x
- 7. B. Bammens, P. Evenepoel, K. Verbeke and Y. Vanrenterghem, *Am. J. Kidney Dis.*, 44 (2004) 278. https://doi.org/10.1053/j.ajkd.2004.04.03
- 8. S. Suresh and U. B. R. Ragula, *Mater. Today*, 24(2020)723.

- https://doi.org/10.1016/j.matpr.2020.04.
- 9. T. Kameda, K. Horikoshi, S. Kumagai, Y. Saito and T. Yoshioka, *J. Chem. Eng.*, 28 (2020) 2993. https://doi.org/10.1016/j.cjche.2020.03.0 18
- 10. K. Namekawa, M. T. Schreiber, T. Aoyagi and M. Ebara, *Biomater. Sci.*, 2 (2014) 674. https://doi.org/10.1039/C3BM60263J
- 11. T. Panasyuk-Delaney, V. M. Mirsky and O. S. Wolfbeis, *Electroanalysis*, 14 (2002) 221. https://doi.org/10.1002/1521-4109(200202)14:3%3C221::AID-ELAN221%3E3.0.CO;2-Y
- 12. Q. Zhao, M. Seredych, E. Precetti, C. E. Shuck, M. Harhay, R. Pang, C.-X. Shan and Y. Gogotsi, *ACS Nano*, 14 (2020) 11787.
 - https://doi.org/10.1021/acsnano.0c04546
- C.-H. Ooi, W.-K. Cheah and F.-Y. Yeoh, *Adsorption*, 25 (2019) 1169.

 https://doi.org/10.1007/s10450-019-00130-5
- Y. Bai, Y. Dou, L.-H. Xie, W. Rutledge, J.-R. Li and H.-C. Zhou, *Chem. Soc.Rev.*, 45 (2016) 2327. https://doi.org/10.1039/C5CS00837A
- 15. C. Cabello-Alvarado, M. Andrade-Guel, D. Medellin-Banda, C. Ávila-Orta, G. Cadenas-Pliego, A. Sáenz-Galindo, R. Radillo-Radillo, J. Lara-Sánchez and L. Melo-Lopez, *Mater. Lett.*, 320 (2022)132382.
 - https://doi.org/10.1016/j.matlet.2022.132382
- 16. P.H. Lolekha, S. Jaruthunyaluckand P. Srisawasdi. *J. Clin. Lab. Anal.*, 15, (2001)121.
 - https://doi.org/10.1002/jcla.1013
- 17. S.Manzoor, T.M. Ansari, M.Arslan, A.Intizar, A. Fatima, M. Mujahid and M.A.Hanif, *Int. J. Environ. Anal. Chem.*, 102(2022) 2415. https://doi.org/10.1080/03067319.2020.1756276

- 18. M. Arslan, S. Manzoor, T. M. Ansari, A. Yar, S. Naz, A. Yousaf and G. Yasmin, *Desalin. Water Treat.*,109 (2018)175. https://doi.org/10.5004/dwt.2018.22083
- 19. J. Simon Craw, Matthew D. Cooper and Ian H. Hillier, *J. Chem. Soc.*, 2 (1997) 869. https://doi.org/10.1039/A608586E
- 20. T.Bell, Z. Hou, Y.Luo and M. Drew, *Science*, 269 (1995) 671. https://doi.org/10.1126/science.7624796
- 21. D. B. Lefranc, H. Pizzala, R. Denoyel, V. Hornebecq, J. L.B. Lefranc and R. Guieu, *Micropor. Mesopor. Mat.*, 119 (2009) 186. https://doi.org/10.1016/j.micromeso.2008.10.016
- 22. R. Reddick and G. Kenyon, *J. Am. Chem. Soc.*, 109 (1987) 4380. https://doi.org/0002-7863/87/1509-4380S01.50/0
- 23. W. K. Chen, C. H. Lu, J. Xu, Y. C. Yang and J. Q. Li, *J. Struct. Chem.*, 21 (2002) 190. https://doi.org/10.47176/ijpr.21.3.38481

- 24. G. Baojiao, P. Jiang and Haibo Lei, *Mater. Lett.*, 60 (2006) 3404. https://doi.org/10.1016/j.matlet.2006.03.
- 25. M. Schreierand J. R. Regalbuto, *J. Catal.*, 225 (2004) 202. https://doi.org/10.1016/j.jcat.2004.03.034.
- 26. G. H. Wang, L. Q. Yongand S. C. Hua, *Anal. Methods*, 19 (2014) 7847. https://doi.org/10.1039/C4RA05111D
- 27. S. Ding, Z. Tonghui, L. Peiyun and W. Xuefen, *J. Membr. Sci.*, 636 (2021) 119550. https://doi.org/10.1016/j.memsci.2021.1 19550
- 28. J. Ju, F. Liang, X. Zhang, R. Sun, X. Pan, X. Guanand M. Li, *Chin. J. Chem. Eng.*, 27 (2019) 1383. https://doi.org/10.1016/j.cjche.2019.01.022
- 29. C. Grundahl, H. Kishwar, J. Rosenberg, M. Jensen, A. Laursen, W. Sørensen and J. Thomas, *ACS Sens.*, 3(2019) 692. https://doi.org/10.1021/acssensors.8b000 24